

Research on Fuzzy Enhancement in the Diagnosis of Liver Tumor from B-mode Ultrasound Images

Wu Qiu, Feng xiao, Xin Yang, Xuming Zhang, Ming Yuchi, Mingyue Ding

School of Life Science and Technology,
Key Laboratory of Image Processing and Intelligent Control of Education Ministry of China
Huazhong University of Science and Technology, Wuhan, Hubei, China
kyobati@gmail.com

Abstract—Fuzzy enhancement is applied in computer aided diagnosis of liver cancer from B mode ultrasound images as a pre-processing procedure in this paper. It was evaluated with three classifiers including K means, back propagation neural network and support vector machine using 25 features from first order statistic (FOS), gray-level co-occurrence matrix (GLCM), gray-level run-length matrix (GLRLM), Grey level dependant matrix (GLDM) and LAWS. In the analysis of 166 normal liver tissue, 30 hemangioma and 60 malignant tumor, our method improved the classification accuracy of three classifiers (K means, BP neural network and support machine vector) in distinguishing liver cancer, hemangioma and normal liver cancer from B mode ultrasound images. It is proved that fuzzy enhancement as an efficient preprocessing procedure could be used in the computer aided diagnosis system of liver cancer.

Index Terms—fuzzy enhancement, liver cancer, neural network, support vector machine, computer aided diagnosis

I. INTRODUCTION

Liver cancer is one of the most popular malignant tumors in Asia. In patients with chronic viral infection, the severity of the disease may be ranked from asymptomatic healthy carriers to patients with cirrhosis of the liver[1-3]. The gold standard for diagnosis of patients with diffuse parenchyma liver diseases depends primarily on a needle biopsy of the liver. However, the pathological measurement of diseases such as hepatitis and liver cirrhosis may be severely biased due to the sampling error in the biopsy specimen. B-mode ultrasound diagnosis is the first option in popular diagnostics due to its economy, efficiency, noninvasiveness. Affected by the quality of ultrasound images of liver cancer, benign expression of malignant tumors and observer's visual fatigue, careless mistakes, and diagnostic level, not all liver cancers can be detected accurately. Thus, it's necessary to provide the medical operators a computer aided diagnosis (CAD) system which is helpful to reduce the possibility of wrong diagnosis or missed diagnosis[4-6].

According to the ultrasound image representation of hepatocellular carcinoma (HCC) and echo type in the tumors, there are five types of primary carcinoma of liver, which are corresponding to low echo type, equal echo type, high echo type, mixed echo type and diffuse type respectively. Most CAD systems are based on texture features which are extracted from the B mode ultrasound

images. These features are used to classify three sets of ultrasonic liver images-normal liver, hepatoma, and cirrhosis. Texture features include the spatial gray-level dependence matrices, the Fourier power spectrum, the gray-level difference statistics, and the Laws' texture energy measures [7-9]. Classifiers include Bayes classifier, K means, neural network[6,10], support vector machine (SVM)[11,12], et al. However, the accuracy of classification is greatly affected by quality of the ultrasound images. Ultrasound images quality are greatly effected by the ultrasound machine settings and the operation of operators which directly affect the classification accuracy.

In this paper, we aim to use fuzzy enhancement to preprocess the input ultrasound images in order to decrease the effect resulted from different ultrasound machine settings in the computer aided diagnosis of liver cancer from ultrasound images. According to the characteristic of B-mode ultrasonic liver image, we will compare the classification accuracy of different classifiers with the fuzzy enhancement [13,14] used in processing of images. The classifiers in this paper include K-means, back-propagation neural network, SVM.

II. METHODS

The object of enhancement technique is to process a given image so that the result is more robust than the original for classification of liver cancer. The methods so far developed for image enhancement may be categorized in two broad classes, namely, frequency-domain methods and spatial-domain methods. The technique in the first category is based on modifying the Fourier transform of an image, whereas in spatial domain methods the direct manipulation of the pixel is adopted. The technique used here is based on the modification of pixels in the fuzzy property plane of an image. The property domain is extracted from the spatial domain using fuzzifiers which play the role of creating different amounts of fuzzification in the plane. The fuzzy operator, contrast intensification, is taken as a tool for enhancement.

A. Fuzzy feature plane

Define $\Omega=\{X\}$ is a set, $\mu_D(x)$ is a function of each element in Ω where $0 \leq \mu_D(x) \leq 1$. $\mu_D(x)$ is used describe the subjection of X to D. D is a fuzzy set of Ω and $\mu_D(x)$ is subjection function of D. According to the concept of fuzzy subset, a $M \times N$ image X with L grey

levels can be considered as a fuzzy points set , denoted as ,

$$X = \begin{bmatrix} p_{11} / x_{11} & p_{12} / x_{12} & \cdots & p_{1N} / x_{1N} \\ p_{21} / x_{21} & p_{22} / x_{22} & \cdots & p_{2N} / x_{2N} \\ \cdots & \cdots & \cdots & \cdots \\ p_{M1} / x_{M1} & p_{M2} / x_{M2} & \cdots & p_{MN} / x_{MN} \end{bmatrix} \quad (1)$$

OR

$$\bigcup_{i=1}^M \bigcup_{j=1}^N p_{ij} / x_{ij} \quad (i = 1, 2, \dots, M; j = 1, 2, \dots, N) \quad (2)$$

Where p_{ij} describe the state that the pixel (i, j) has the feature $P_{ij} (0 \leq P_{ij} \leq 1)$. P_{ij} is called fuzzy feature. If the comparative grey level of the pixel is considered as the interest fuzzy feature, and x_{ij} is the grey level of pixel (i, j) , X_{\max} is the maximum grey level in the image, the fuzzy feature can be explained as follows,

$$P_{ij} = F(x_{ij}) = [1 + (\frac{x_{\max} - x_{ij}}{F_p})^2]^{-1} \quad (i = 1, 2, \dots, M; j = 1, 2, \dots, N) \quad (3)$$

Where F_p is fuzzy parameter. Eq 3 shows that when

$x_{ij} \rightarrow X_{\max}$, $P_{ij} \rightarrow 1$; when x_{ij} decreases ,

P_{ij} decreases correspondingly. Therefore, fuzzy

feature P_{ij} denotes the possibility that the pixel (i, j) has the maximum grey level. The plane composed by all P_{ij} , $(i = 1, 2, \dots, M; j = 1, 2, \dots, N)$ is called fuzzy feature plane. when $x_{ij} = 0$, P_{ij} is a finite positive number,

$$P_{ij} = [1 + (\frac{x_{\max}}{F_p})^2]^{-1} \quad (4)$$

The range of P_{ij} is $[\alpha, 1]$.

B. Model of fuzzy enhancement

If the contrast enhancement operator CEO which is applied on the fuzzy set D can produce a new fuzzy set $CEO(D) = D'$, its subsection function is expressed as:

$$\mu_{D'}(x) = \mu_{CEO(D)}(x) = \begin{cases} 2[\mu_D(x)]^2 & (0 \leq \mu_D(x) \leq 0.5) \\ 1 - 2[1 - \mu_D(x)]^2 & (0.5 \leq \mu_D(x) \leq 1) \end{cases} \quad (5)$$

This operation decreases the fuzzification of fuzzy set D, and increases the value of $\mu_D(x)$ when it is more than 0.5, decreases the value of $\mu_D(x)$ when it is less

than 0.5. We can use transformation T_1 to denote the operation above,

$$\mu_{D'}(x) = T_1(\mu_D(x)) = \begin{cases} T_1^{(1)}(\mu_D(x)) & (0 \leq \mu_D(x) \leq 0.5) \\ T_1^{(2)}(\mu_D(x)) & (0.5 \leq \mu_D(x) \leq 1) \end{cases} \quad (6)$$

When the Eq 6 is applied on the fuzzy feature plane, then

$$P'_{ij}(x) = T_k(P_{ij}) = \begin{cases} T_k^{(1)}(P_{ij}) & (0 \leq P_{ij} \leq 0.5) \\ T_k^{(2)}(P_{ij}) & (0.5 \leq P_{ij} \leq 1) \end{cases} \quad (7)$$

Where T_k can be regarded as the iterations of T1. when $k \rightarrow \infty$, $T_k(P_{ij})$ will produce a binary image. If T_k is iterated with finite times, the image can be enhanced obviously. The detailed of fuzzy enhancement algorithm in this paper can be described as,

(1) Extract the fuzzy feature of image, and constitute the fuzzy feature plane : $P_{ij} = F(x_{ij})$.

(2) On the fuzzy feature plane, use contrast enhancement transformation T_k to enhance fuzzy feature P_{ij} and obtain the fuzzy enhanced P'_{ij} .

(3) Apply inverse transformation on the new fuzzy feature plane to get the enhanced output images $x'_{ij} = F^{-1}(P'_{ij})$.

Considering $P_{ij} \in [\alpha, 1]$, plane P_{ij} possibly contains the region where P'_{ij} is less than α . all the value of P'_{ij} is replace as α when P'_{ij} is less than α , its corresponding constraint condition is denoted as $\alpha \leq P_{ij} \leq 1$, which is the constraint condition of inverse transformation. In the process of fuzzy enhancement, suitable fuzzy parameter F_p is important to the enhancement result, which is related to critical point X_c in the image space, X_c should satisfy the following conditions:

$$\begin{aligned} x_{ij} &> X_c, P_{ij} > 0.5, \\ x_{ij} &< X_c, P_{ij} < 0.5. \end{aligned} \quad (8)$$

We can change the enhancement result through adjusting the fuzzy parameter F_p . In our application , critical point X_c is empirically less than the half of the average grey level of the image.

III. EXPERIMENTAL METHODS

The experimental procedure is described as the Fig 1. The subimage including region of interest (ROI) was extracted manually from the acquired liver ultrasound images firstly. Then fuzzy enhancement was applied to improve the subimage quality. Texture features were extracted to train and test the classifiers.

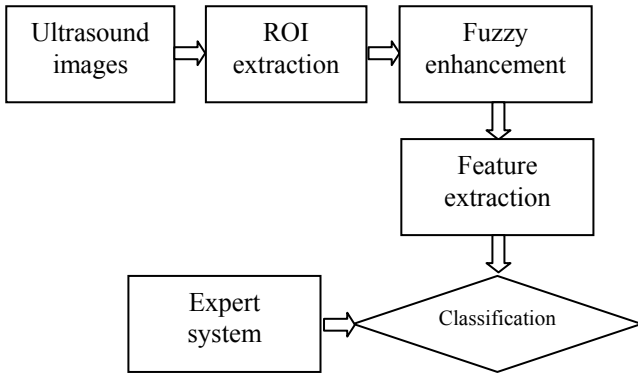


Fig.1 The flow chart of the processing

A. Image acquisition

A total of 256 sonograms from patients, including 60 liver cancers (malignant (MAL)), 30 hemangioma (HEM) and 166 normal liver tissue (NOR), which were divided into two groups. 30 liver cancer images, 31 hemangioma images and 83 normal liver images were used as training dataset, and the rest are used for testing.

B. Determination of ROI

To reduce the impact of translation of the focal region, a focal region in the liver cancer image were selected manually by physicians since the size of focal region in different images are different. For example, the tumor in low echo liver cancer images is always small, but in high echo liver cancer images is large. This should cause the size of our region of interest (ROI) became variable. The size of each image is 90*93 with 256 gray levels in our experiments. The effect of size of the regions to the classification accuracy was reported in our previous experiments[2]. The size of region is empirically determined as 30*30 pixels larger than the usual size of liver tumor in this study.

C. Feature extraction method

In order to validate the method, we used the original ultrasound images and fuzzy enhancement processed images to do the experiments. 25 features from first order statistic (FOS), gray-level co-occurrence matrix (GLCM), gray-level run-length matrix (GLRLM) and Gray level difference matrix (GLDM) were extracted from the

ultrasound images[15]. These features are regarded as the input of the classifiers.

(1) FOS

The first order statistical features employed in this research were as follows:

$$1) \text{ Mean: } \mu = \sum_{i=0}^{L-1} iP(i)$$

$$2) \text{ Standard deviation: } \sigma^2 = \sum_{i=0}^{L-1} (i - \mu)^2 P(i)$$

$$3) \text{ Skewness: } s = \frac{1}{\sigma^3} \sum_{i=0}^{L-1} (i - \mu)^3 P(i)$$

$$4) \text{ Kurtosis: } K = \frac{1}{\sigma^4} \sum_{i=0}^{L-1} (i - \mu)^4 P(i)$$

$$5) \text{ Energy: } ENERGY = \sum_{i=0}^{L-1} [P(i)]^2$$

$$6) \text{ Entropy: } ENT = -\sum_{i=0}^{L-1} P(i) \log[P(i)]$$

(2) GLCM

1) Moment of inertia:

$$ASM = \sum_h \sum_k m_{hk}^2$$

2) Energy:

$$CON = \sum_h \sum_k (h - k)^2 m_{hk}$$

3) Entropy:

$$ENT = -\sum_h \sum_k m_{hk} \log m_{hk}$$

4) Correlation coefficient:

$$COR = \frac{\sum_h \sum_k hkm_{hk} - \mu_x \mu_y}{\sigma_x \sigma_y}$$

m_{hk} is the appearing frequency of pairs of pixels, which has grey level of h and k respectively. $\mu_x, \mu_y, \sigma_x, \sigma_y$ 分别 are the mean and standard deviation of m_h and m_k respectively, here, $m_k = \sum_h m_{hk}$ $m_h = \sum_k m_{hk}$.

(3) GLRLM

1) Short run emphasis:

$$SRE = \frac{\sum_{g=1}^{N_g} \sum_{l=1}^{N_l} (m_{gl} / l^2)}{\sum_{g=1}^{N_g} \sum_{l=1}^{N_l} m_{gl}}$$

2) Long run emphasis:

$$LRE = \frac{\sum_{g=1}^{N_g} \sum_{l=1}^{N_l} (l^2 m_{gl})}{\sum_{g=1}^{N_g} \sum_{l=1}^{N_l} m_{gl}}$$

3) Gray level nonuniformity:

$$GLN = \frac{\sum_{g=1}^{N_g} (\sum_{l=1}^{N_l} m_{gl})^2}{\sum_{g=1}^{N_g} \sum_{l=1}^{N_l} m_{gl}}$$

4) Run length nonuniformity:

$$RLN = \frac{\sum_{l=1}^{N_l} (\sum_{g=1}^{N_g} m_{gl})^2}{\sum_{g=1}^{N_g} \sum_{l=1}^{N_l} m_{gl}}$$

5) Run percentage:

$$RP = \frac{\sum_{l=1}^{N_l} \sum_{g=1}^{N_g} m_{gl}}{P}$$

(4) Grey level dependant matrix (GLDM)

We consider here a class of local properties based on absolute differences between the gray levels of pixels in the ROI. Let $I(x, y)$ be the image intensity function. For any given displacement $\delta = (\Delta x, \Delta y)$, let $I_\delta(x, y) = |I(x, y) - I(x + \Delta x, y + \Delta y)|$, and $f(i | \delta)$ be the probability density of $I_\delta(x, y)$. The value of $f(i | \delta)$ is obtained from the number of times $I_\delta(x, y)$ occurs for a

given δ , i.e. $f(i | \delta) = P(I_\delta(x, y) = i)$. If a texture is directional, the degree of spread of the values in $f(i | \delta)$ should vary with the direction of δ , given that its magnitude is in the proper range. Thus, texture directionality can be analyzed by comparing spread measures of $f(i | \delta)$ for various directions of δ . In the present study, four possible forms of the vector δ were considered: $(0, d)$, $(d, 0)$, $(-d, d)$, and $(-d, -d)$, with d being the interpixel distance, each of which corresponds to a displacement in vertical, horizontal, 135° and 45° direction, respectively. From each of the density functions corresponding to one of the above-mentioned

directions, five texture features were obtained:

1) Contrast: $con = \sum_i i^2 f(i | \delta)$

2) Mean: $mn = \sum_i i f(i | \delta)$

3) Entropy: $ent = -\sum_i f(i | \delta) \log f(i | \delta)$

4) Inverse difference moment:

$$idm = \sum_i \frac{f(i | \delta)}{i^2 + 1}$$

5) Angular second moment:

$$asm = \sum_i [f(i | \delta)]^2$$

(5) LAWS

Laws developed the texture energy features using the following 1D kernels: $L=[1,6,15,20,15,6,1]$, $E=[-1,-4,-5,0,5,4,1]$, $S=[-1,-2,1,4,1,-2,-1]$, $W=[-1,0,3,0,-3,0,1]$, $R=[1,-2,-1,4,-1,-2,1]$, $O=[-1,6,-15,20,-15,6,-1]$, where, L, E, S, W, R, and O denote level, edge, spot, wave, ripple, and oscillation, respectively. The texture energies from the following kernels are typically computed. Using these 1D kernels of length seven, 2D convolution kernels are generated by convolving a vertical 1D kernel with a horizontal 1D kernel. Five texture features were obtained.

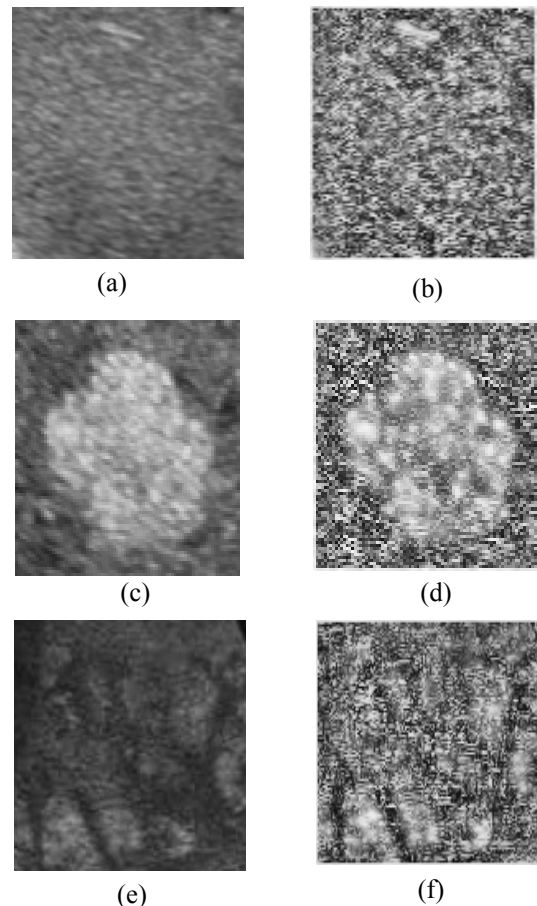


Figure. 1 Results of fuzzy enhancement

IV. RESULTS

In our experiments, three classifiers including K means, back propagation (BP) neural network (NN), support vector machine (SVM) were compared so as to evaluate the influence of fuzzy enhancement on the different classifiers.

A. Experimental result of fuzzy enhancement

One of results of fuzzy enhancement are shown in Figure.1. The left columns are original images. (a) is normal liver tissue image, (c) is hemangioma image and (e) is liver cancer image. The right columns in Figure 1 are their corresponding images processed by fuzzy enhancement.

B. K means experimental results

Table.1 Classification result of liver cancer from normal liver tissue with K means.

	Original images	Fuzzy enhancement processed images
sensitivity	50%(15/30)	56.67%(17/30)
1 - specificity	69.39%(68/98)	75.51%(74/98)

Table.2 Classification result of liver cancer from hemangioma and normal liver tissue with K means.

	Original images	Fuzzy enhancement processed images
sensitivity	60%(18/30)	73.33%(22/30)
1 - specificity	78.31%(65/83)	87.95%(73/83)

Firstly K means [16] was used to differentiate liver cancer from normal liver tissue and liver cancer from abnormal liver (liver cancer and hemangioma). The results are showed in Table 1 and Table 2 respectively. Then we used K means to classify images into three classes, normal liver tissue, liver cancer and hemangioma. Table 3 shows the three classes result. The results show that fuzzy enhancement can improve the classification accuracy of K means in these three experiments although the classification sensitivity of K means is not high.

Table 3 Three classes result with K means.

	Original images	Fuzzy enhancement processed images
Liver cancer	33.33%(20/60)	41.67% (25/60)

Normal liver	56.02%(93/166)	57.83% (96/166)
Hemangioma	40% (12/30)	36.67% (11/30)

B. BP neural network experimental results

We did the same experiments as K means using BP NN[17]. The target error we defined in our BP neural network is 0.01. With this target error our NN method can get the best classification accuracy in our experiments. However, if the value of target error is too small, the convergence rate is slow and it is easy to result in over-training. If the error is too big, the approximation is not accurate. Table 4 and Table 5 show the classification results of differentiating liver cancer from normal liver tissue and liver cancer from abnormal liver respectively. Three classes result with BP NN is shown in Table 6. The results demonstrate that fuzzy enhancement method can improve the classification accuracy of BP NN although BP NN can obtain good classification sensitivity without fuzzy enhancement.

Table 4 Classification result of liver cancer from normal liver tissue with BP NN.

	Original images	Fuzzy enhancement processed images
sensitivity	93.33%(28/30)	96.67%(29/30)
1 - specificity	97.59%(81/83)	98.79%(82/83)

Table 5 Classification result of liver cancer from hemangioma and normal liver tissue with BP NN.

	Original images	Fuzzy enhancement processed images
sensitivity	93.33%(28/30)	93.33%(28/30)
1 - specificity	97.96%(96/98)	95.92%(94/98)

Table 6 Three classes result with BP neural network

	Original images	Fuzzy enhancement processed images
Liver cancer	93.33% (28/30)	93.33% (28/30)
Normal liver	96.39% (80/83)	98.79% (82/83)
Hemangioma	86.67% (13/15)	86.67% (13/15)

C. SVM experimental results

Table 7 Classification result of liver cancer from normal liver tissue with SVM

	Original images	Fuzzy enhancement processed images
sensitivity	96.67%(29/30)	100%(30/30)
1 - specificity	98.79%%(82/83)	98.79%(82/83)

Table 8 Classification result of liver cancer from hemangioma and normal liver tissue with SVM

	Original images	Fuzzy enhancement processed images
sensitivity	93.33%(28/30)	93.33%(28/30)
1 - specificity	98.98%(97/98)	98.98%(97/98)

Table 9 Three classes result with SVM

	Original images	Fuzzy enhancement processed images
Liver cancer	96.67%(29/30)	100%(30/30)
Normal liver	98.79%(82/83)	96.39% (80/83)
Hemangioma	80%(12/15)	93.33%(14/15)

We used polynomial kernel function to implement the SVM[18]. The punishment coefficient C is assigned 1000 and parameter γ and d are assigned 1 and 3 respectively in our experiments. Table 7, Table 8 and Table 9 show the classification results of SVM. The results show that SVM

can get the best classification accuracy compared to the K means and BP neural network. Since SVM can differentiate liver cancer well from normal liver tissue, or from hemangioma and normal liver tissue, image preprocessing, such as fuzzy enhancement processing, can not improve the classification accuracy effectively when SVM was used to classify two classes (Table 7 and Table 8). However, when SVM was applied to classify three classes, the classification accuracy with fuzzy enhancement increase from 96.67% to 100%, for liver cancer, from 80% to 93.33% for hemangioma (Table 9).

V. DISCUSSION AND CONCLUSION

In this paper, the fuzzy enhancement algorithm was applied to computer aided diagnosis of liver cancer ultrasound images. 25 features from first order statistic (FOS), gray-level co-occurrence matrix (GLCM), gray-level run-length matrix (GLRLM), Grey level dependant matrix (GLDM) and LAWS were extracted to train the different classifiers. The results with K means, BP neural network and SVM show that SVM can obtain the best classification accuracy, K means can not be regarded as a robust classifier to differentiate liver cancer from normal liver tissue and hemangioma in B mode ultrasound images. The experimental results with fuzzy enhancement demonstrate that it can improve classification accuracy of three classifiers. It is concluded that fuzzy enhancement can be used as an efficient preprocessing procedure in the computer aided diagnosis of liver cancer. Future work includes that more subject images could be used to evaluate the efficiency of the algorithm.

ACKNOWLEDGMENT

The authors wish to thank Maolin Ye, Rui Wang, Kaitong Li. This work was supported in part by a grant from National Nature Science Foundation of China (30911120497, 61001141, 60975011), China Postdoctoral Science Foundation (20100480906), and Fundamental Research Funds for the Central Universities under the grants of HUST (2010JC036).

REFERENCES

- [1] H. Yoshida, D. D Casalino, B. Keserci, A. Coskun, O. Ozturk and A.Savranlar: "Wavelet-packet-based texture analysis for differentiation between benign and malignant liver tumours in ultrasound images". *Phys. Med. Biol.*(48),3735-3753,2003.
- [2] M.E. Mayerhoefer, M.Breitenseher,G.Amannd, and M. Dominkus. "Are signal intensity and homogeneity useful parameters for distinguishing between benign and malignant soft tissue masses on MR images? Objective evaluation by means of texture analysis". *Magnetic Resonance Imaging*, 26(9),1316-1322,2008.
- [3] G Xian. "An identification method of malignant and benign livertumors from ultrasonography based on GLCM texture features and fuzzy SVM". *Expert Systems with Applications*, (37), 6737-6741,2010.
- [4] K Doi, "Computer-aided diagnosis in medical imaging: Historical review, current status and future potential",

Computerized Medical Imaging and Graphics, 31, 198–211, 2007.

- [5] S. Huang, M. Ding, “Feature Statistic Analysis of Ultrasound Images of Liver Cancer”. Proc of SPIE. 8(48), 6789ON, Nov, 2007.
- [6] K.Mala, V.Sadasivam, and S.Alagappan, “Neural Network based Texture Analysis of Liver Tumor from Computed Tomography Images”, International Journal of Biological and Medical Sciences, (21), 33-41, 2007.
- [7] S. K. Kakkos, J. M. Stevens, A. N. Nicolaides, E. Kyriacou, C. S. Pattichis, G. Geroulakos, and D. Thomas, “Texture analysis of ultrasonic images of symptomatic carotid plaques can identify those plaques associated with ipsilateral embolic brain infarction,” Eur. J. Vasc. Endovasc Surg. **33**, 422–429, 2007.
- [8] J. Awad and A. Krasinski, “Texture analysis of carotid artery atherosclerosis from three-dimensional ultrasound images”, Medical Physics, 37(4), 1382-1392, 2010.
- [9] C. I. Christodoulou, C. S. Pattichis, M. Pantziaris, and A. Nicolaides, “Texture-based classification of atherosclerotic carotid plaques,” IEEE Trans. Med. Imaging **22**, 902–912, 2003.
- [10] J Liu, H.B Chang, T.Y. Hsu and X Ruan. Prediction of the flow stress of high-speed steel during hot deformation using a BP artificial neural network. Journal of Materials Processing Technology. 103(2),200-205,2000.
- [11] C. Cortes, V Vapnik. “Support-Vector Network” .Machine Learning , 20, 273-297,1995.
- [12] N.D.Freitas, “Sequential Support Vector Machines” .Neural Networks for Signal Processing IX, 1 , 31-40,1999.
- [13] G S Tzafestas, S N Raptis. “Image segmentation via iterative fuzzy clustering based on local spacefrequency multi-feature coherence criteria”. Journal of Intelligent and Robotic Systems,28(1), 21-37,2000.
- [14] H D Cheng, Y H Chen, Y Sun, “A novel fuzzy entropy approach to image enhancement and thresholding”. Signal Processing,75(3), 277-301,1999.
- [15] J. Awad , A. Krasinski,G. Parraga and A. Fenster. “Texture analysis of carotid artery atherosclerosis from three-dimensional ultrasound images”. Med.Phys. 37(4),1382-1392,2010.
- [16] K. Wagsta, C. Cardie, S. Rogers and S. Schroedl. “Constrained K-means Clustering with Background Knowledge”. Proceedings of the Eighteenth International Conference on Machine Learning, p. 577-584, 2001.
- [17] J Liu, H.B Chang, T.Y. Hsu and X Ruan. “Prediction of the flow stress of high-speed steel during hot deformation using a BP artificial neural network”. Journal of Materials Processing Technology. 103(2),200-205,2000.
- [18] A.Mathur and G.M.Foody. “Multiclass and Binary SVM Classification:Implications for Training and Classification Users”. IEEE Geoscience and remote sensing letters,5(2),241-245, 2008.



in the school of Life science and technology in HUST. His

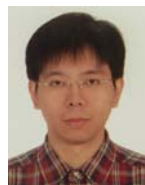
Wu Qiu was born in Hunan, China, on June 14, 1981. He received his B.S. and M.S. degrees in material processing engineering from Huazhong University of Science and Technology(HUST), the Ph.D. degree in pattern recognition and artificial intelligence from HUST. He is now working as a post doctor

current research interests include 3D ultrasound application, medical image processing, pattern recognition et al.



Xuming Zhang was born in Hubei Province, China. He received the B.S. and M.S. degrees in Material Science and Engineering from Wuhan University of Technology, in 1998 and 2001, respectively. He obtained the Ph.D. degree in Material Science and Engineering from Shanghai Jiaotong University in 2005.

During 2006 and 2008, he was a postdoctoral researcher in the State Key Lab of Digital Equipment and Technology at HUST. From 2008 to 2009, he undertook his postdoctoral research in the Department of Mechanical and Aerospace Engineering at University of California, Davis. He is currently associate professor in the School of life science and technology at HUST. His research interests are medical imaging, image processing and computer vision.



Ming Yuchi received his Ph.D. in Electrical Engineering from Korea Advanced Institute of Science and Technology, Daejeon, in February 2006 and his M.S. in Power Electronics, from Gyeongsang National University, Jinju, in June 2000 respectively in Republic of Korea. He graduated from HUST, Wuhan, China with B.S. in Automatic Control Engineering in June 1997.

He is currently an Associate Professor in School of Life Science and Technology, HUST, Wuhan, China since October 2007. And he worked for School of Information and Communication Technology Gold Coast Campus, Griffith University Queensland, Australia as a Postdoctoral Research Fellow from July 2006 to July 2007.

His major fields of studies are biomedical engineering, ultrasound, evolutionary computation, fuzzy system as a member of IEEE.



Mingyue Ding was born in Sichuan, China on May 13, 1961. He received his Bachelor Degree in electronic engineering in 1982 from Beijing University of Aerospace and Aeronautics, Beijing, China. In 1985, he received his Master Degree in communication and electronic system from Chinese University of Electronic Science and Technology, Chengdu, Sichuan, China. He got his Doctoral Degree in communication and electronic system in 1988 from HUST, Wuhan, Hubei, China.

From 1988 to 2000, he was a lecturer, associate professor and full professor at the Institute for Pattern Recognition and Artificial Intelligence, HUST. From 2000 to 2005, he was a researcher associate in Robarts Research Institute, The University of Western Ontario, London, Ontario, Canada. Currently he is the chairman and full professor of Department of Bio-medical Engineering, HUST, Wuhan, Hubei, China. More than 7 books and 300 academic papers were published by him and his students.

Prof. Ding is the senior member of IEEE and member of SPIE. He received an Alexander von Humboldt Fellowship from Germany in 1991 and was awarded a Canadian Creative Award in 2001.